Published in final edited form as:

Mol Cancer Res. 2021 May ; 19(5): 862–873. doi:10.1158/1541-7786.MCR-20-0915.

Palbociclib renders human papilloma virus-negative head and neck squamous cell carcinoma vulnerable to the senolytic agent navitoclax

Nicholas J. Gadsden[1], **Cory D. Fulcher**[2], **Daniel Li**[3], **Nitisha Shrivastava**[4], **Carlos Thomas**[4], **Jeffrey E. Segall**[4,5], **Michael B. Prystowsky**[4], **Nicolas F. Schlecht**[4,6,7,8], **Evripidis Gavathiotis**[7,9,10], **Thomas J. Ow**[2,4]

[1]Department of Anesthesiology, Columbia University, New York, NY, USA.

[2]Department of Otorhinolaryngology - Head and Neck Surgery, Montefiore Medical Center / Albert Einstein College of Medicine, Bronx, NY, USA.

[3]Medical Student, Montefiore Medical Center / Albert Einstein College of Medicine, Bronx, NY, USA.

[4]Department of Pathology, Montefiore Medical Center / Albert Einstein College of Medicine, Bronx, NY, USA.

[5]Department of Department of Anatomy & Structural Biology, Montefiore Medical Center / Albert Einstein College of Medicine, Bronx, NY, USA.

[6]Division of Oral Health and Society, Faculty of Dentistry, McGill University, Montreal, Canada.

[7]Department of Epidemiology and Population Health, Montefiore Medical Center / Albert Einstein College of Medicine, New York, United States

[8]Department of Cancer Prevention and Control, Roswell Park Comprehensive Cancer Center, Buffalo, NY, USA

[9]Department of Biochemistry, Albert Einstein College of Medicine, Bronx, NY, USA.

[10]Department of Medicine (Cardiology), Albert Einstein College of Medicine, Bronx, NY, USA.

Abstract

We demonstrate that inhibition of cyclin dependent kinases 4/6 (CDK4/6) leads to senescence in human papillomavirus (HPV)-negative (−) head and neck squamous cell carcinoma (HNSCC), but not in HPV-positive (+) HNSCC. The BCL-2 family inhibitor, navitoclax, has been shown to eliminate senescent cells effectively. We evaluated the efficacy of combining palbociclib and navitoclax in HPV- HNSCC. Three HPV- HNSCC cell lines (CAL27, HN31, PCI15B) and three HPV+ HNSCC cell lines (UPCI-SCC-090, UPCI-SCC-154, UM-SCC-47) were treated with palbociclib. Treatment drove reduced expression of phosphorylated Rb (p-Rb) and phenotypic

Corresponding Author: Thomas J. Ow, MD, MS, 3rd Floor Medical Arts Pavilion, 3400 Bainbridge Avenue, Bronx, NY 10467, Phone: (718) 920-8488, thow@montefiore.org.

Conflict of Interest Statement

The authors declare no potential conflicts of interest.

evidence of senescence in all HPV- cell lines, while HPV+ cell lines did not display a consistent response by Rb or p-Rb and did not exhibit morphologic changes of senescence in response to palbociclib. In addition, treatment of HPV- cells with palbociclib increased both β-galactosidase protein expression and BCL-xL protein expression compared to untreated controls in HPV- cells. Co-expression of p-galactosidase and BCL-xL occurred consistently indicating elevated BCL-xL expression in senescent cells. Combining palbociclib with navitoclax led to decreased HPV- HNSCC cell survival and led to increased apoptosis levels in HPV- cell lines compared to each agent given alone.

Keywords

Head and neck squamous cell carcinoma; senescence; apoptosis; palbociclib; navitoclax

INTRODUCTION

Head and neck squamous cell carcinoma (HNSCC) accounts for approximately 90 percent of all cases of head and neck malignancy [1], and there are an estimated 53,000 new cases of HNSCC diagnosed in the United States each year, with more than 10,000 deaths occurring annually [2]. Approximately two-thirds of patients are diagnosed with advanced stage disease upon initial presentation [3,4] and these patients require an aggressive multi-modality treatment approach including surgery, radiation, and cisplatin-based chemotherapy. Despite aggressive treatment, there remains high morbidity and mortality [5], with a 30 percent rate of locoregional recurrence, distant failure in 25 percent of patients, and five-year survival of approximately 40 percent [6,7].

Loss of normal cell cycle regulation is a hallmark of HNSCC [8]. With human papillomavirus positive (HPV+) disease, the viral oncoproteins E6 and E7 produced by HPV lead to the functional inactivation of the p53 and Rb tumor suppressor proteins, respectively. This disruption allows unchecked progression of the cell cycle, even while the *CDKN2A* gene, which encodes the p16INK4A (p16) cell cycle inhibitor, remains intact [9,10]. In HPV-negative (HPV-) disease, loss or inactivation of *CDKN2A*/p16 is an early and common event in HNSCC tumorigenesis, with disruption of this gene occurring in 58% of cases [11]. P16 is immediately upstream of cyclin dependent kinase 4 and 6 (CDK4/6). Loss of functional p16 allows CDK4/6 to complex with D-type cyclins in order to phosphorylate and inactivate Rb, leading to release of E2F and subsequent progression through the G1 checkpoint to the S phase of the cell cycle [9,12,13]. Loss of regulation of this critical checkpoint leads to cell cycle dysregulation and unchecked cell proliferation.

These key genomic and molecular differences between HPV+ and HPV- HNSCC lead to squamous cancers with different clinical behavior and responses to therapy [14,15]. HPV+ HNSCC is primarily located in the oropharynx, most often occurs in younger and healthier patients, and carries a much better prognosis compared to HPV- disease, which occurs in an older population and tends to be associated with tobacco or alcohol use [16–18]. Because of these differences, molecularly targeted treatment strategies should be tailored to the specific biologic and genomic characteristics inherent to these HNSCC subtypes. As outcomes

among patients with HPV- HNSCC are substantially worse, there is a specific unmet need for improved strategies among these patients.

Targeting CDK4/6 with specific inhibitors seems to be a logical strategy in HPV- HNSCC. We hypothesized that HPV- HNSCC cells would be more sensitive to CDK4/6 inhibition than HPV+ HNSCC given the key molecular differences between the two HNSCC subtypes. Palbociclib, a selective CDK4/6 inhibitor, has already been approved by the Federal Drug Administration (FDA) for the treatment of estrogen receptor (ER)-positive and HER2-negative advanced/metastatic breast cancer. CDK4/6 inhibitors have been shown to arrest cell cycle progression beyond the G1 phase, promoting either cellular quiescence or senescence [19–23]. However, senescent cells undergo significant changes in their gene expression profile, many of which are pro-tumorigenic [24,25]. Specifically, senescent tumor cells have been shown to upregulate pro-survival pathways and inhibit apoptosis to maintain survival [26–28]. Senescent tumor cells that persist in the tumor microenvironment have been shown to resist traditional cytotoxic chemotherapy and secrete cancer-promoting signals [29]. Clearing senescent cells would reduce the ability of those cells to promote a pro-tumorigenic microenvironment. Thus, a treatment strategy combining the senescence-promoting effects of CDK4/6 inhibitors with an additional modality that could exploit the vulnerabilities of senescent cells and lead to their selective elimination would be beneficial [30]. ‘Senolytic agents’, which selectively kill senescent cells, have gained recent interest. ABT-263 (Navitoclax), which targets the BCL-2, BCL-xL, and BCL-w pro-survival proteins [31], is a known senolytic drug [32]. We hypothesized that inducing a senescent-like state with CDK4/6 inhibition would sensitize HPV- HNSCC cells to senolytic treatment with navitoclax.

In this study, we demonstrate that CDK4/6 inhibition with palbociclib in HPV- HNSCC cells consistently induces a senescent state, with upregulation of the pro-survival BCL-2 family protein, BCL-xL. The induction of senescence is absent in HPV+ HNSCC cells, demonstrating that the approach is specific to the HPV- HNSCC molecular subtype. Further, we show that coupling navitoclax with palbociclib results in profound apoptosis in HPV- HNSCC cells.

MATERIALS AND METHODS

Cell Culture

HNSCC cell lines CAL27, UPCI-SCC-090, and UPCI-SCC-154 were obtained from the American Type Culture Collection (ATCC), and the cell lines HN31, PCI15B, and UM-SCC-47 were obtained from a repository maintained by Jeffrey N. Myers, MD, PhD, at the University of Texas, MD Anderson Cancer Center, with additional required permissions (HN31: John Ensley, MD, Wayne State University; PCI15B: Jennifer Grandis, MD, University of Pittsburgh; UM-SCC-47: Thomas Carey, PhD, University of Michigan). All cells were maintained in Dulbecco’s Modified Eagle’s Medium (DMEM), except for UPCI-SCC-154, which was grown in Minimum Essential Eagle’s Medium (MEM). All media were supplemented with 10% Fetal Bovine Serum (FBS), non-essential amino acids, sodium pyruvate, and 1% antibiotic: penicillin / streptomycin (DMEM) or gentamicin (MEM). The cells were incubated at 37°C and 5% CO_2, with all experimentation performed within 20 passages after thawing frozen stock cells. Stock samples for all cell lines were authenticated

with short tandem repeat (STR) genotyping immediately prior to the establishment of bank samples for each cell line for experimental use. Cells obtained from ATCC (CAL27, UPCI-SCC-090, and UPCI-SCC-154) were reported *Mycoplasma* tested by ATCC prior to receipt and establishment of bank samples for experimental use. Cells obtained from a repository maintained by Jeffrey N. Myers, MD, PhD, (HN31, PCI15B, and UM-SCC-47) were similarly *Mycoplasma* tested prior to receipt and establishment of stocks. In addition, before stock samples were frozen, all cells were treated with Plasmocure™ (InvivoGen, San Diego, CA) per manufacturer specifications. Samples were used for experiments after recovery from freezing (within 2–3 passages) and were not extended for experiments beyond 20 passages. All lines utilized for this study were authenticated subsequent to experimentation using STR genotyping to confirm they remained valid.

Antibodies

Antibodies against β-actin (8H10D10), β-galactosidase (E2U2I), BCL-2 (124), BCL-xL (54H6), BCL-w (31H4), and phosphorylated retinoblastoma (Ser780) protein (9307S) were obtained from Cell Signaling Technology (Danvers, MA). Antibody against retinoblastoma protein (MA5-11387) (Thermo Fisher Scientific, Waltham, MA) was also obtained.

Drugs

Palbociclib was obtained from Selleck Chemicals (PD-0332991; Houston, TX) and dissolved in water. Navitoclax was also obtained from Selleck Chemicals (S1001; Houston, TX) and dissolved in dimethyl sulfoxide (DMSO). Any time navitoclax was used in the treatment condition, the control condition was treated with a proportional amount of DMSO as the vehicle-control.

Western Blot

Cells were seeded and incubated with palbociclib 1μM for 24 hours. This dosage was utilized to measure distinct molecular changes, and the early timepoint was required to capture cells before cell death occurred. Cells were lysed using radioimmunoprecipitation (RIPA) buffer containing protease and phosphatase inhibitors (Pierce, Thermo Fisher Scientific, Rockford, IL). Protein concentrations of the cell lysates were determined by DC Protein Assay (Bio-Rad Laboratories, Hercules, CA). Protein samples were loaded onto 10% polyacrylamide gels in equivalent amounts and separated by electrophoresis at 80V, then transferred onto polyvinylidene fluoride (PVDF) membranes (Merck Millipore, Burlington, MA) overnight at 4°C at 35V. The membranes were blocked in 1% Bovine Serum Albumin in Tris-buffered saline with 0.1% Tween 20 (Thermo Fisher Scientific, Waltham, MA) and probed with several primary antibodies overnight at 4°C, including antibodies against β-actin, phosphorylated retinoblastoma protein, and retinoblastoma protein. All primary antibodies were diluted at 1:500 in 1% BSA/TBS-T, except for β-actin, which was used as a loading control protein and was diluted 1:5000 in 1% BSA/TBS-T. The membranes were washed and probed for 1 hour with the following fluorescent secondary antibodies: IRDye goat anti-mouse IgG and IRDye goat anti-rabbit IgG (LI-COR Biosciences, Lincoln, NE), which were diluted 1:2500 in 1% BSA/TBS-T. The membranes were washed again prior to the visualization of immunoreactive proteins using the LI-COR Odysey FC Imaging System (LI-COR Biosciences, Lincoln, NE).

When evaluating β-galactosidase and the BCL-2 family proteins, the cells were incubated with Palbociclib 1μM for 48 hours prior to harvesting. Here, the primary antibodies utilized were β-galactosidase, BCL-2, BCL-xL, and BCL-w. All of these primary antibodies were diluted 1:500 in 1% BSA/TBS-T. After incubation with secondary antibody and visualization of the immunoreactive proteins, quantification of protein bands was performed using Image Studio software (LI-COR Biosciences, Lincoln, NE). Experimental data is comprised of at least three biological replicates performed on different days.

Cellular Morphology Assessment

Cellular morphology was observed in the HNSCC lines with and without treatment with palbociclib 1μM. Brightfield microscopy images were taken on day of drug addition (day 0), then day 3 and day 5 of incubation in drug-treated media. Incubation with palbociclib was continued throughout the 5-day period, with media and drug replaced at 72 hours.

Real-time Imaging of HNSCC Cells Treated with Palbociclib

Time-lapse videos were captured using the Personal Automated Lab Assistant (PAULA) (Leica Microsystems, Wetzlar, Germany). Cells were plated and observed with and without administration of palbociclib 1μM treatment. 24 hours after drug administration, videos were recorded at 15-minute intervals for 48 hours. Videos were processed using HitFilm Express software and compressed into 10 second videos.

Clonogenic Assay

Cells were treated with palbociclib 0.05μM, 0.1μM, or 0.5μM. Palbociclib doses used in the clonogenic survival assays were reduced as compared to western blot or immunofluorescence assays in order to observe measurable differences in cell viability using this assay, which by design requires drug treatment of cells plated at low density over a course of several days. Plates were assessed for clonal expansion, with replacement of media and drug every 72 hours. After approximately 10 days (CAL27, HN31, PCI15B, UM-SCC-47), or 14 days (UPCI-SCC-090 and UPCI-SCC-154), media was removed, and plates were washed. Cells were fixed and stained with 0.25% Cresyl Violet. Plates were scanned and the results were quantified with ImageJ software [33], with a colony defined as consisting of at least 50 cells [34]. Plating efficiency was calculated for each cell line, and surviving fractions were determined per standard methods [34]. Statistical significance was determined using ANOVA and Dunnett's multiple comparisons test comparing treatment conditions to control, which was calculated with GraphPad Prism 8 (GraphPad Software, San Diego, CA). For a pooled analysis of all HPV+ lines compared with all HPV- lines, each treatment condition was compared to control using matched-pairs t-tests. Experimental data is comprised of three biological replicates performed on different days, with three technical replicates per biological replicate.

Immunofluorescence

Cells were seeded onto cover slips and were treated with palbociclib 1μM or DMEM for 48 hours prior to fixation with 4% paraformaldehyde in PBS (Santa Cruz Biotechnology, Dallas, TX). Cover slips were washed, incubated with 0.1% Triton-X (Fischer Scientific,

Fair Lawn, NJ), and blocked in 5% BSA in TBS-T. Next, the cover slips were probed with primary antibody overnight at 4°C: β-galactosidase (1:400 in 1% BSA/TBS-T with 0.3% Triton-X) or BCL-xL (1:200 in 1% BSA/TBS-T with 0.5% n-octyl-glucoside), followed by probing with fluorescent secondary antibody. Secondary antibodies were diluted 1:500 in 1% BSA/TBS-T and were either anti-rabbit IgG Alexa Fluor 488 (4412) (Cell Signaling Technology, Danvers, MA) or anti-rabbit IgG Alexa Fluor 647 (ab150079) (Abcam, Cambridge, MA). The cover slips were then washed and mounted with Antifade Mounting Medium with DAPI (Enzo Life Sciences, Farmingdale, NY). The slides were examined utilizing an epifluorescent microscope, ZEISS AxioObserver CLEM, with DAPI, Alexa 488, or Cy5 fluorescent filters. For each cell line and condition, 5 representative fields were captured, with each field containing approximately 100 cells. The total fluorescent signal from each field was quantified using Volocity Software (Quorum Technologies, Puslinch, ON) and normalized by the number of cells within that field. A two-tailed t-test was calculated comparing the control and treatment groups. Finally, the averages of the amounts of signal per cell were compared in order to quantify the fold change in the amount of fluorescent signal. Experimental data is comprised of at least three biological replicates performed on different days.

Confocal Microscopy

For dual color visualization of β-galactosidase and BCL-xL, we utilized antibody against β-galactosidase diluted 1:400, and BCL-xL Alexa Fluor 546 antibody (sc-8392 AF546) (Santa Cruz Biotechnology, Dallas, TX) diluted 1:200. Both were diluted in 1% BSA/TBS-T with 0.3% Triton-X. After overnight incubation at 4°C, cover slips were washed and probed with fluorescent secondary antibody, anti-rabbit IgG Alexa Fluor 488 (4412) (Cell Signaling Technology, Danvers, MA), for 2 hours at room temperature. The cover slips were then washed and mounted with Antifade Mounting Medium with DAPI (Enzo Life Sciences, Farmingdale, NY). The slides were examined utilizing a Leica SP5 Confocal microscope, with 405 nanometer, 488 nanometer, and 543 nanometer lasers. For each cell line and condition, 5 representative fields were captured, with each field containing approximately 100 cells. 10 cells were selected from identical XY coordinates in each field, and the fluorescent signal from each channel was quantified using FIJI Image J software [35]. The fluorescent signal values were normalized by the median of each experimental replicate. All values were plotted, and a Pearson correlation coefficient was calculated with GraphPad Prism 8 (GraphPad Software, San Diego, CA). Experimental data is comprised of at least three biological replicates performed on different days.

Cell Viability Assay

Cells were seeded and treated 24 hours after plating with palbociclib 0.5μM, navitoclax 1μM, or a combination of the two. Vehicle-treated control wells were maintained in the DMSO dissolvent for navitoclax. The cells were incubated in drug for a total of 144 hours, with replacement of cell media after the first 72 hours. Cells were then washed and stained with 0.25% Cresyl Violet. Plates were scanned and the results were quantified with ImageJ software [33]. The percentage of cresyl violet staining in relation to the total surface area of the well was used to estimate cell density for each well as a measure of cell number, and data was normalized to vehicle-treated control wells. Statistical significance was determined

by two-tailed paired t-tests, calculated comparing the control and combination treatment groups, as well as comparing single-treated and combination treatment groups. Experimental data is comprised of three biological replicates performed on different days, with three technical replicates per biological replicate.

Annexin V Apoptosis Assay

Cells were seeded and treated with palbociclib 0.5μM, navitoclax 1μM, or palbociclib 0.5μM / navitoclax 1μM combination, as well as the positive control, staurosporine 1μM (AdipoGen Life Sciences, San Diego, CA). Vehicle-treated control wells were maintained in DMSO of the same proportion as used in the treatment condition. Cells were incubated for 72 hours in drug. Media and any detached cells were harvested from wells and included in the analysis. Attached cells were harvested with Accutase Cell Detachment Solution (BD Biosciences, San Jose, CA), and combined with the media from each respective well. All cells were washed and stained with the PE Annexin V Apoptosis Detection Kit I (BD Biosciences, San Jose, CA). Analysis was performed using a flow cytometer, BD LSRII UP. Flow cytometer data was analyzed using FlowJo software (FlowJo, Ashland, OR). Experimental data comprised of three biological replicates performed on different days. Statistical significance was determined using two-tailed paired t-tests comparing the combination treatment group with each single agent treatment groups for each line.

Statistical Analysis

All experiments comprised of at least three assays performed independently on different days. Mean average, standard deviation (SD), or standard error of the mean (SEM) was calculated where appropriate. Statistical significance was calculated with unpaired t-tests, unless otherwise indicated, and a two-sided p-value < 0.05 was considered statistically significant. Other analyses or statistical methods utilized for specific assays are detailed in their respective sections in the methods.

RESULTS

Initial experiments were performed using six HNSCC lines, including 3 HPV- lines (CAL27, HN31, and PCI15B) and 3 HPV+ lines (UM-SCC-47, UPCI-SCC-090, UPCI-SCC-154). The origin of each line is described in more detail in Table 1. HPV-16 infection has been confirmed in UM-SCC-47[36], UPCI-SCC-090[37], and UPCI-SCC-154[37] and reported as negative for CAL27, HN31, and PCI15B[36].

Effects of Palbociclib

To demonstrate the molecular activity of palbociclib we assessed protein levels of total Rb and phosphorylated Rb at baseline and after 24 hours of exposure to palbociclib 1μM for all cell lines. In the HPV- cell lines, phosphorylation of Rb was markedly reduced after palbociclib treatment, while there was no observable change in the level of Rb phosphorylation in the three HPV+ cell lines, as shown in Supplemental Figure 1.

Using light microscopy, we observed that the cellular morphology of HPV- cells following exposure to palbociclib is dramatically altered. Figure 1a reveals that with palbociclib

exposure, HPV- cell lines undergo flattening and enlargement, and appear grossly to proliferate at a slower rate in comparison to untreated cells, all of which are characteristic features of cellular senescence [24,25]. These morphological changes are not present in the HPV+ cell lines with or without palbociclib treatment, and the cells appear to proliferate at a similar rate under both conditions, as seen in Figure 1b. These striking differences are also demonstrated on real-time imaging of these cells provided as Supplemental Files linked to this manuscript. One can clearly see that HPV- cells treated with palbociclib lack cell division and appear to enlarge as compared to untreated controls, while HPV+ cells exhibit similar proliferation and gross morphology in both treated and untreated conditions.

To further assess the cellular response to palbociclib, clonogenic survival was measured after treatment with palbociclib, as displayed in Figure 2a and 2b. HPV- cell lines were significantly more susceptible to palbociclib than the HPV+ cell lines, once again illustrating a differential effect of palbociclib based upon HPV status. At palbociclib 0.5 pM, surviving fraction (mean percent ± SEM) compared to control was decreased among HPV- cell lines (CAL27: 0% ± 0%, HN31: 51.89% ± 3.96%, PCI15B: 3.35% ± 1.08%), and comparatively less effective in HPV+ cell lines (UM-SCC-47: 77.67% ± 5.22%, UPCI-SCC-090: 116.89% ± 9.85%, UPCI-SCC-154: 72.28% ± 3.84%). Analysis pooling data for HPV+ and HPV- lines demonstrated clear differential responses to palbociclib between the two HNSCC molecular sub-types (Figure 2c).

To verify that the palbociclib-treated cells with morphological features of senescence were in a senescent state, we assessed senescence associated β-galactosidase (SA β-Gal) activity, a known surrogate marker for cellular senescence [24,25,38,39]. As displayed in Figure 3a and 3b, SA β-Gal expression was significantly increased after treatment with palbociclib in the HPV- cell lines. This result was corroborated using immunofluorescence, when significantly increased SA β-Gal expression was visualized in palbociclib-treated HPV- cell lines in comparison to untreated controls (Figure 3d and 3e).

Expression of Pro-Survival / Anti-Apoptotic Proteins

After observing the molecular and cellular response to palbociclib, as well as noting the pattern of differential response based upon HPV- status, we then focused on HPV- HNSCC. We hypothesized that palbociclib-induced senescence would result in the upregulation of pro-survival BCL family proteins based on previous reports that senescent cells demonstrate increased BCL-xL levels [26–28]. Baseline protein expression levels of three pro-survival / anti-apoptotic proteins, BCL-2, BCL-xL, and BCL-w, (molecules targeted by the senolytic agent, navitoclax) were measured using western blot and compared to expression levels following 48 hours of treatment with 1 μM palbociclib. BCL-2 and BCL-w appeared to be absent or very low in both the untreated and treated conditions for all lines tested (Supplemental Figure 2). Thereafter, BCL-xL was examined in subsequent experiments. Quantification of BCL-xL demonstrated significantly increased expression levels in all HPV- cell lines when treated with palbociclib (Figure 3a and 3c). We utilized immunofluorescence to evaluate if there was a subset of cells upregulating BCL-xL in response to palbociclib treatment, or if this response was consistent across all treated cells. The upregulation of BCL-xL in response to 48 hours of 1 μM palbociclib treatment was widely distributed across

the population, of a significant increase, and consistent across all HPV- cell lines (Figure 3f and 3g).

Next, we hypothesized that individual cells affected by palbociclib treatment would respond by concurrently increasing expression levels of both SA β-Gal and BCL-xL. Conversely, cells that were relatively unaffected by palbociclib treatment would have lower levels of SA β-Gal and BCL-xL. Using confocal microscopy and co-expression analysis, Figure 4a–f illustrates that intracellular levels of β-Gal and BCL-xL levels correlate strongly for all of the cell lines examined.

Targeting Pro-Survival / Anti-Apoptotic Proteins as a Senolytic Approach

Since HPV- HNSCC cells appear to upregulate BCL-xL following palbociclib treatment, we hypothesized that this was a protective mechanism to resist cell death. As such, we hypothesized that inhibiting BCL-xL in HPV- HNSCC cells treated concurrently with palbociclib would result in profound apoptosis. ABT-263 (navitoclax) is a specific inhibitor of the anti-apoptotic BCL-2 family proteins, BCL-2, BCL-xL, and BCL-w [31]. Cell viability assays using cresyl violet were used to assess the response of HPV- HNSCC cells to the combination of palbociclib and navitoclax treatment. In comparison to treatment with either agent alone, the combination of the two agents led to significantly lower levels of viable cells (Figure 5).

Senolysis via Induction of Apoptosis

To determine the method of cell death following drug exposure, we assayed apoptosis using Annexin V and 7-AAD following treatment with palbociclib alone, navitoclax alone, or after concurrent treatment. We hypothesized that navitoclax would induce cell death by apoptosis in the palbociclib treated senescent-like cells. Combination treatment of palbociclib and navitoclax significantly increased levels of apoptosis when compared to treatment with either single agent palbociclib or navitoclax (Figure 6). In fact, combination treatment of palbociclib and navitoclax reached levels of apoptosis that were similar to the positive control, staurosporine.

DISCUSSION

In this study, we demonstrate that HPV- HNSCC cells respond consistently to the CDK4/6 inhibitor palbociclib. This response was largely absent among HPV+ HNSCC lines. We observed that palbociclib is biologically active in HPV- lines through a decrease in phosphorylated Rb, and these cells appeared to undergo senescence based on consistent morphologic changes and increased expression of SA-βGal. Examination of BCL-2 family pro-survival proteins showed that HPV- HNSCC cells increase expression of BCL-xL in response to palbociclib-induced senescence. We further studied a novel combination treatment strategy for HPV- HNSCC that utilizes palbociclib as a sensitizer for the senolytic agent, navitoclax. Navitoclax is a specific inhibitor of the anti-apoptotic BCL-2 family proteins that is currently undergoing evaluation in multiple clinical trials, however none are focused on HNSCC [31,40]. Our proof-of-concept study shows that palbociclib treated HPV- HNSCC cells undergo senescence and seem to upregulate BCL-xL to maintain cell survival.

We show that combining navitoclax with palbociclib leads specifically to profound levels of apoptotic cell death in HPV- HNSCC.

HNSCC has now been clearly stratified into two distinct entities based on HPV-status, as evidenced by newly established staging criteria for HPV+ oropharynx cancer and HPV- disease[17]. Cell cycle disruption is a key hallmark in HNSCC, but, as already discussed, the means by which this is accomplished between HPV- and HPV+ HNSCC are starkly different. The *CDKN2A* gene and/or the function of its product, p16INK4A, is lost in over 80% of HPV- HNSCC tumors [11]. Molecular inhibitors of CDK4/6, in effect, re-establish p16 function, providing a rationale for their utility in this setting. Because the downstream cell cycle regulator, Rb, is disrupted by the E7 oncoprotein in HPV+ HNSCC, one would expect CDK4/6 inhibition to be ineffective. This is indeed what we observed. There was a subtle response to palbociclib noted in 2 HPV+ cell lines, particularly at higher doses of palbociclib, but these responses were limited in contrast to the HPV- lines, suggesting the primary action may be secondary to Rb activity. It is true that CDK4/6 signal on downstream targets other than Rb, such as FOXM1 [41], which may contribute to responses to palbociclib in both HPV+ and HPV- HNSCC. We plan to detail the mechanism of response in HNSCC to inhibition of CDK4 and CDK6 in more comprehensive future studies. Our current study is the first to our knowledge to demonstrate the activity of CDK4/6 inhibitors in both HPV- and HPV+ HNSCC in a series of proof-of-concept experiments across multiple HNSCC cell lines. Our results provide support for a biomarker-driven strategy based on HPV status that is potentially effective in HNSCC.

Overall, there is insufficient data examining CDK4/6 inhibition in HNSCC, either in preclinical or clinical work [42]. A study by Gong and colleagues described that among a large panel of cancer cell lines subjected to CDK4/6 inhibition with abemaciclib, with 28 HNSCC lines among this panel (including CAL27, but no other overlapping lines), there were modest responses overall [43]. Unlike the study by Gong et al., we specifically focused on HNSCC and compared HPV- and HPV+ lines. Similar to the findings of Gong and colleagues, the responses to palbociclib alone that we observed were modest and limited to HPV- lines only. It is also notable that abemaciclib has more selectivity for CDK4, which may have implications for reduced activity in HNSCC [44,45].

In general, because palbociclib is an anti-proliferative, cytostatic agent, it is often most effective in eliminating cancer cells when used in combination with other drugs [19,46,47.] For instance, palbociclib is approved for treatment of ER+/HER2- breast cancer in combination with anti-estrogen therapy [48]. Two preclinical studies in HNSCC have shown improved results when CDK4/6 inhibitors are combined with a second agent [49,50]. and multiple clinical trials evaluating CDK4/6 inhibitors in combination with additional agents are currently underway, including a study examining palbociclib and cetuximab in HNSCC [30,51,52]. While CDK4/6 inhibition as a part of a combination strategy has high potential as an effective treatment in HNSCC, the ideal agents to combine in HNSCC remain yet to be established [42]. This motivated our interest in targeting specific biological vulnerabilities among HPV- HNSCC when exposed to palbociclib.

Consistent but limited activity in HNSCC led us to examine combining a rationally effective agent with palbociclib. We chose the senolytic agent, navitoclax. There are limited data studying navitoclax in HNSCC. At the time of writing this manuscript, there are a total of 5 active trials studying navitoclax registered on clinicaltrials.gov, with several more that are not yet recruiting patients. No trials are specifically studying this agent in HNSCC. Most studies are focused either on lymphoproliferative disease, hematologic cancers, or in the treatment of myelofibrosis. Trials in solid tumors focus mostly on either lung cancers or any tumor with recurrent/metastatic disease. Trials studying combination navitoclax with molecularly targeted agents include agents targeting mTOR (NCT03366103), EGFR (NCT02520778), or other RAS pathway targets (NCT02079740, NCT01989585). No trials have explored combining CDK4/6 inhibitors with navitoclax. Notably, several trials are focused on examining the senolytic properties of navitoclax to combat fibrosis. We thus hypothesized that the senescence we observed in HPV- HNSCC cells after palbociclib treatment might increase the cancer cells' susceptibility to navitoclax.

Palbociclib treatment appears to consistently induce senescence in HPV- HNSCC. Our findings are in accord with what has been seen previously described in other cancer models, where CDK4/6 inhibitors halt progression beyond G1 phase and promote either a transient quiescent state or permanent proliferative arrest in senescence [19–23]. The cytostatic and senescence-inducing nature of CDK4/6 inhibition may underly the limited effects of CDK4/6 inhibitors as monotherapeutic agents. Our knowledge of the role that senescent cancer cells play in tumor biology and treatment response continues to evolve, and it is now thought to potentially contribute to both tumor suppression and tumor progression [24,29]. One biological phenomenon that has been recently described is that the senescent state can lead to the upregulation of pro-survival BCL-2 family proteins [26–28]. It is known that the relative abundance and balance between pro-survival and pro-apoptotic members of the BCL-2 family helps determine cell survival, and it seems that senescent cancer cells may rely on these molecules to persist in the senescent state [28,53]. We found that this to be particularly important in HPV- HNSCC. Recent work by our laboratory has suggested that anti-apoptotic BCL-2 family proteins BCL-xL and MCL-1 are overexpressed in HNSCC, and that targeting these proteins results in synergistic cell death [54]. Our previous work, combined with our current study, suggests that palbociclib may exacerbate the dependence of HPV- HNSCC on BCL-xL.

BCL-2 family pro-survival proteins are well known to influence tumorigenesis and tumor progression in cancer, and they appear to influence cell fate between senescence and apoptosis [55]. For example, colorectal cancer cells that would normally undergo drug-induced senescence following treatment with a topoisomerase I inhibitor, instead undergo apoptosis when first subjected to BCL-xL knockdown [56]. A study by Zhu et al. also showed that siRNA silencing of BCL-xL expression selectively killed senescent cells [27]. Work by Yosef et al. showed that cells that have become senescent (either by etoposide treatment, extensive replication, or oncogene expression) upregulate BCL-xL, and that inhibition of BCL-xL in these senescent cells by either siRNA or ABT-737 specifically induces apoptosis *in vitro* [32]. They further showed that *in vivo,* ABT-737, an early analogue of navitoclax, eliminates senescent cells that had accumulated in the lungs of mice following radiation [32]. Pan et al. illustrated that navitoclax selectively cleared senescent pneumocytes following lung

radiation, and demonstrated that ABT-263 treatment reversed pulmonary fibrosis several months after irradiation [57]. Finally, Chang et al. showed that ABT-263 selectively targeted and induced apoptosis in bone marrow hematopoietic stem cells that had been induced to senescence by irradiation, subsequently promoting the expansion of the remaining normal hematopoietic stem cells and allowing rejuvenation of the hematopoietic system [58]. This body of research supports a potential dual role for senolytic therapy as a strategy to treat cancer, eliminating senescent cells while protecting host organ systems from the toxicity of cytotoxic agents. Our work supports the efficacy of this strategy in HNSCC and warrants closer evaluation in both *in vivo* and clinical studies.

Targeting and eliminating senescent cells has become an area of growing interest [59]. Cancer cells can undergo senescence following exposure to cytotoxic chemotherapy, allowing them to serve as a reservoir for sustained pro-tumorigenic signaling, which enhances the surrounding cells' tumorigenic potential and leads to relapses and metastases [60–62]. Additionally, persistent senescent cells contribute to a local and systemic inflammatory state, exacerbating both the side effects of chemotherapy and the premature aging and frailty seen in cancer survivors [60,61]. Clearing senescent cells is especially relevant in HNSCC, given that treatment currently relies on cytotoxic cisplatin chemotherapy combined with radiotherapy. Radiotherapy induces cellular senescence, and persistent senescent cells can create a chronic inflammatory state that ultimately contributes to fibrosis in the tissues of the irradiated field [63,64]. Those same persistent cells may also facilitate tumor relapse and metastasis [63,64]. Given that senescence is a known resistance mechanism and cause of treatment morbidity in HNSCC, a strategy targeting and eliminating senescent cells in this setting would therefore fill an unmet need, improving both treatment efficacy while possibly decreasing toxicity.

To our knowledge, we are the first to report a strategy combining the induction of senescence by CDK4/6 inhibition with the specific senolytic clearance of those senescent cells by targeting anti-apoptotic BCL-2 family proteins with navitoclax. This study presents a preliminary exploration of the potential of this dual-agent combination. We acknowledge several limitations of this work. Though we confirmed our findings across several HNSCC lines, broader evaluation in a larger panel of cell lines with more widely characterized molecular and genomic alterations is warranted to establish clear biomarkers for response to our proposed therapeutic strategy. We plan to expand our future evaluation to a larger cell line panel and translational models (e.g. primary tumor cell cultures) to accomplish these goals. Despite this limitation, our work suggests that in HNSCC response to palbociclib is dependent on HPV status, and we are the first to leverage a pervasive molecular characteristic (loss of p16 function) to design a senolytic treatment strategy for this disease. We further acknowledge that this study does not include demonstration of efficacy and toxicity of the palbociclib and navitoclax combination *in vivo.* These studies are planned in our ongoing work.

In conclusion, this preclinical *in vitro* study provides significant insight into the underlying biology of HPV- HNSCC. These cancers appear to be susceptible to palbociclib-induced senescence that depends on BCL-xL, which then leads to an inherent vulnerability to navitoclax. Our proof-of-concept work is the first describe this approach in HNSCC. Future

studies that optimize this biomarker-driven strategy in HPV- HNSCC are warranted, as the current strategies to treat this disease continue to lead to high morbidity and a consistent rate of treatment failure.

Supplementary Material

Refer to Web version on PubMed Central for supplementary material.

ACKNOWLEDGEMENTS

The authors would like to acknowledge the contributions of members of the Analytical Imaging Facility (Andrea Briceno, Hillary Guzik, Vera DesMarais) and of the Flow Cytometry Core Facility (Jinghang Zhang, Aodeng Aodengtuya) at the Albert Einstein College of Medicine.

Financial Support

Thomas J. Ow's contribution was supported in part by the NIH-NIDCR grant K23 DE027425. The authors also acknowledge support from the Albert Einstein Cancer Center (NIH-NCI P30CA013330), specifically the flow cytometry core facility, part of the Albert Einstein shared resources and the Department of Pathology. The manuscript content is solely the responsibility of the authors and do not necessarily represent the official views of the National Institute of Health (NIH).

REFERENCES

1. Pfister D, Ang K, Brizel D, Burtness B, Cmelak A, Colevas A. Head and neck cancers. Journal of the National Comprehensive Cancer Network. 2011;9(6):596–650. [PubMed: 21636536]
2. Siegel RL, Miller KD, Jemal A. Cancer statistics, 2019. CA Cancer J Clin. 2019;69(1):7–34. [PubMed: 30620402]
3. Pedruzzi PAG, Kowalski LP NI, Oliveira BV, Tironi F, Ramos GH. Analysis of prognostic factors in patients with oropharyngeal squamous cell carcinoma treated with radiotherapy alone or in combination with systemic chemotherapy. Archives of Otolaryngology--head & neck surgery. 2008;134(11): 1196–1204. [PubMed: 19015451]
4. Argiris A, Karamouzis MV, Raben D, Ferris RL. Head and neck cancer. The Lancet. 2008;371(9625):1695–1709.
5. Furness S, Glenny AM, Worthington HV, et al. Interventions for the treatment of oral cavity and oropharyngeal cancer: chemotherapy. Cochrane Database of Systematic Reviews. 2011(4).
6. Cooper JS, Pajak TF, Forastiere AA, et al. Postoperative Concurrent Radiotherapy and Chemotherapy for High-Risk Squamous-Cell Carcinoma of the Head and Neck. New England Journal of Medicine. 2004;350(19):1937–1944.
7. Pignon JP, Bourhis J, Domenge C, Designé L. Chemotherapy added to locoregional treatment for head and neck squamous-cell carcinoma: three meta-analyses of updated individual data. The Lancet. 2000;355(9208):949–955.
8. Leemans CR, Braakhuis BJM, Brakenhoff RH. The molecular biology of head and neck cancer. Nature Reviews Cancer. 2011;11(1):9–22. [PubMed: 21160525]
9. Tornesello Maria PF, Buonaguro L, Ionna F, Buonaguro FM, Caponigro F. HPV-related oropharyngeal cancers: from pathogenesis to new therapeutic approaches. Cancer letters. 2014;351(2):198–205. [PubMed: 24971935]
10. Chung CH, Gillison ML. Human Papillomavirus in Head and Neck Cancer: Its Role in Pathogenesis and Clinical Implications. Clinical Cancer Research. 2009;15(22):6758. [PubMed: 19861444]
11. Lawrence MS, Sougnez C, Lichtenstein L, et al. Comprehensive genomic characterization of head and neck squamous cell carcinomas. Nature. 2015;517(7536):576–582. [PubMed: 25631445]
12. Verschuren EW, Jones N, Evan GI. The cell cycle and how it is steered by Kaposi's sarcoma-associated herpesvirus cyclin. J Gen Virol. 2004;85(Pt 6): 1347–1361. [PubMed: 15166416]

13. Solomon B, Young RJ, Rischin D. Head and neck squamous cell carcinoma: Genomics and emerging biomarkers for immunomodulatory cancer treatments. Semin Cancer Biol. 2018;52(Pt 2):228–240. [PubMed: 29355614]
14. Ang KK, Harris J, Wheeler R, et al. Human papillomavirus and survival of patients with oropharyngeal cancer. N Engl J Med. 2010;363(1):24–35. [PubMed: 20530316]
15. Salazar CR, Anayannis N, Smith RV, et al. Combined P16 and human papillomavirus testing predicts head and neck cancer survival. Int J Cancer. 2014;135(10):2404–2412. [PubMed: 24706381]
16. Mehanna H, Jones TM, Gregoire V, Ang KK. Oropharyngeal carcinoma related to human papillomavirus. Bmj. 2010;340:c1439. [PubMed: 20339160]
17. Lydiatt WM, Patel SG, O'Sullivan B, et al. Head and Neck cancers-major changes in the American Joint Committee on cancer eighth edition cancer staging manual. CA Cancer J Clin. 2017;67(2):122–137. [PubMed: 28128848]
18. O'Rorke MA, Ellison MV, Murray LJ, Moran M, James J, Anderson LA. Human papillomavirus related head and neck cancer survival: a systematic review and meta-analysis. Oral Oncol. 2012;48(12):1191–1201. [PubMed: 22841677]
19. Sherr CJ. A New Cell-Cycle Target in Cancer - Inhibiting Cyclin D-Dependent Kinases 4 and 6. The New England journal of medicine. 2016;375(20):1920–1923. [PubMed: 27959598]
20. Baughn LB, Di Liberto M, Wu K, et al. A novel orally active small molecule potently induces G1 arrest in primary myeloma cells and prevents tumor growth by specific inhibition of cyclin-dependent kinase 4/6. Cancer Res. 2006;66(15):7661–7667. [PubMed: 16885367]
21. Michaud K, Solomon DA, Oermann E, et al. Pharmacologic inhibition of cyclin- dependent kinases 4 and 6 arrests the growth of glioblastoma multiforme intracranial xenografts. Cancer Res. 2010;70(8):3228–3238. [PubMed: 20354191]
22. Kovatcheva M, Liu DD, Dickson MA, et al. MDM2 turnover and expression of ATRX determine the choice between quiescence and senescence in response to CDK4 inhibition. Oncotarget. 2015;6(10):8226–8243. [PubMed: 25803170]
23. Puyol M, Martín A, Dubus P, et al. A synthetic lethal interaction between K-Ras oncogenes and Cdk4 unveils a therapeutic strategy for non-small cell lung carcinoma. Cancer Cell. 2010;18(1):63–73. [PubMed: 20609353]
24. Rodier F, Campisi J. Four faces of cellular senescence. J Cell Biol. 2011;192(4):547–556. [PubMed: 21321098]
25. Aravinthan A Cellular senescence: a hitchhiker's guide. Human cell: official journal of Human Cell Research Society. 2015;28(2):51–64.
26. van Deursen JM. Senolytic therapies for healthy longevity. Science (American Association for the Advancement of Science). 2019;364(6441):636–637.
27. Zhu Y, Tchkonia T, Pirtskhalava T, et al. The Achilles' heel of senescent cells: from transcriptome to senolytic drugs. Aging Cell. 2015;14(4):644–658. [PubMed: 25754370]
28. Kirkland JL, Tchkonia T. Cellular Senescence: A Translational Perspective. EBioMedicine. 2017;21:21–28. [PubMed: 28416161]
29. Schosserer M, Grillari J, Breitenbach M. The Dual Role of Cellular Senescence in Developing Tumors and Their Response to Cancer Therapy. Front Oncol. 2017;7:278. [PubMed: 29218300]
30. Klein ME, Kovatcheva M, Davis LE, Tap WD, Koff A. CDK4/6 Inhibitors: The Mechanism of Action May Not Be as Simple as Once Thought. Cancer Cell. 2018;34(1):9–20. [PubMed: 29731395]
31. Tse C, Shoemaker AR, Adickes J, et al. ABT-263: a potent and orally bioavailable Bcl-2 family inhibitor. Cancer Res. 2008;68(9):3421–3428. [PubMed: 18451170]
32. Yosef R, Pilpel N, Tokarsky-Amiel R, et al. Directed elimination of senescent cells by inhibition of BCL-W and BCL-XL. Nat Commun. 2016;7:11190. [PubMed: 27048913]
33. Schneider CA, Rasband WS, Eliceiri KW. NIH Image to ImageJ: 25 years of image analysis. Nature Methods. 2012;9:671. [PubMed: 22930834]
34. Franken NA, Rodermond HM, Stap J, Haveman J, van Bree C. Clonogenic assay of cells in vitro. NatProtoc. 2006;1(5):2315–2319.

35. Schindelin J, Arganda-Carreras I, Frise E, et al. Fiji: an open-source platform for biological-image analysis. Nature Methods. 2012;9:676. [PubMed: 22743772]
36. Zhao M, Sano D, Pickering CR, et al. Assembly and initial characterization of a panel of 85 genomically validated cell lines from diverse head and neck tumor sites. Clin Cancer Res. 2011;17(23):7248–7264. [PubMed: 21868764]
37. White JS, Weissfeld JL, Ragin CC, et al. The influence of clinical and demographic risk factors on the establishment of head and neck squamous cell carcinoma cell lines. Oral Oncol. 2007;43(7):701–712. [PubMed: 17112776]
38. Dimri GP, Lee X, Basile G, et al. A biomarker that identifies senescent human cells in culture and in aging skin in vivo. Proc Natl Acad Sci U S A. 1995;92(20):9363–9367. [PubMed: 7568133]
39. Lee BY, Han JA, Im JS, et al. Senescence-associated beta-galactosidase is lysosomal beta-galactosidase. Aging Cell. 2006;5(2):187–195. [PubMed: 16626397]
40. Suvarna V, Singh V, Murahari M. Current overview on the clinical update of Bcl-2 anti-apoptotic inhibitors for cancer therapy. Eur JPharmacol. 2019;862:172655. [PubMed: 31494078]
41. Anders L, Ke N, Hydbring P, et al. A systematic screen for CDK4/6 substrates links FOXM1 phosphorylation to senescence suppression in cancer cells. Cancer Cell. 2011;20(5):620–634. [PubMed: 22094256]
42. van Caloen G, Machiels JP. Potential role of cyclin-dependent kinase 4/6 inhibitors in the treatment of squamous cell carcinoma of the head and neck. Curr Opin Oncol. 2019;31(3):122–130. [PubMed: 30986809]
43. Gong X, Litchfield LM, Webster Y, et al. Genomic Aberrations that Activate D-type Cyclins Are Associated with Enhanced Sensitivity to the CDK4 and CDK6 Inhibitor Abemaciclib. Cancer Cell. 2017;32(6):761–776.e766. [PubMed: 29232554]
44. Gelbert LM, Cai S, Lin X, et al. Preclinical characterization of the CDK4/6 inhibitor LY2835219: in-vivo cell cycle-dependent/independent anti-tumor activities alone/in combination with gemcitabine. Invest New Drugs. 2014;32(5):825–837. [PubMed: 24919854]
45. Torres-Guzmán R, Calsina B, Hermoso A, et al. Preclinical characterization of abemaciclib in hormone receptor positive breast cancer. Oncotarget. 2017;8(41):69493–69507. [PubMed: 29050219]
46. Sherr CJ, Beach D, Shapiro GI. Targeting CDK4 and CDK6: From Discovery to Therapy. Cancer Discov. 2016;6(4):353–367. [PubMed: 26658964]
47. VanArsdale T, Boshoff C, Arndt KT, Abraham RT. Molecular Pathways: Targeting the Cyclin D-CDK4/6 Axis for Cancer Treatment. Clin Cancer Res. 2015;21(13):2905–2910. [PubMed: 25941111]
48. Finn RS, Martin M, Rugo HS, et al. Palbociclib and Letrozole in Advanced Breast Cancer. N Engl J Med. 2016;375(20):1925–1936. [PubMed: 27959613]
49. Beck TN, Georgopoulos R, Shagisultanova EI, et al. EGFR and RB1 as Dual Biomarkers in HPV-Negative Head and Neck Cancer. Mol Cancer Ther. 2016;15(10):2486–2497. [PubMed: 27507850]
50. Ku BM, Yi SY, Koh J, et al. The CDK4/6 inhibitor LY2835219 has potent activity in combination with mTOR inhibitor in head and neck squamous cell carcinoma. Oncotarget. 2016;7(12):14803–14813. [PubMed: 26909611]
51. Adkins D, Ley J, Neupane P, et al. Palbociclib and cetuximab in platinum-resistant and in cetuximab-resistant human papillomavirus-unrelated head and neck cancer: a multicentre, multigroup, phase 2 trial. Lancet Oncol. 2019;20(9):1295–1305. [PubMed: 31351869]
52. Michel L, Ley J, Wildes TM, et al. Phase I trial of palbociclib, a selective cyclin dependent kinase 4/6 inhibitor, in combination with cetuximab in patients with recurrent/metastatic head and neck squamous cell carcinoma. Oral Oncol. 2016;58:41–48. [PubMed: 27311401]
53. Czabotar PE, Lessene G, Strasser A, Adams JM. Control of apoptosis by the BCL-2 protein family: implications for physiology and therapy. Nat Rev Mol Cell Biol. 2014;15(1):49–63. [PubMed: 24355989]
54. Ow TJ, Fulcher CD, Thomas C, et al. Optimal targeting of BCL-family proteins in head and neck squamous cell carcinoma requires inhibition of both BCL-xL and MCL-1. Oncotarget. 2019;10(4):494–510. [PubMed: 30728900]

55. Childs BG, Baker DJ, Kirkland JL, Campisi J, van Deursen JM. Senescence and apoptosis: dueling or complementary cell fates? EMBO Rep. 2014;15(11):1139–1153. [PubMed: 25312810]

56. Hayward RL, Macpherson JS, Cummings J, Monia BP, Smyth JF, Jodrell DI. Antisense Bcl-xl down-regulation switches the response to topoisomerase I inhibition from senescence to apoptosis in colorectal cancer cells, enhancing global cytotoxicity. Clin Cancer Res. 2003;9(7):2856–2865. [PubMed: 12855666]

57. Pan J, Li D, Xu Y, et al. Inhibition of Bcl-2/xl With ABT-263 Selectively Kills Senescent Type II Pneumocytes and Reverses Persistent Pulmonary Fibrosis Induced by Ionizing Radiation in Mice. Int JRadiat Oncol Biol Phys. 2017;99(2):353–361. [PubMed: 28479002]

58. Chang J, Wang Y, Shao L, et al. Clearance of senescent cells by ABT263 rejuvenates aged hematopoietic stem cells in mice. Nat Med. 2016;22(1):78–83. [PubMed: 26657143]

59. Kirkland JL, Tchkonia T, Zhu Y, Niedernhofer LJ, Robbins PD. The Clinical Potential of Senolytic Drugs. J Am Geriatr Soc. 2017;65(10):2297–2301. [PubMed: 28869295]

60. Short S, Fielder E, Miwa S, von Zglinicki T. Senolytics and senostatics as adjuvant tumour therapy. EBioMedicine. 2019;41:683–692. [PubMed: 30737084]

61. Demaria M, O'Leary MN, Chang J, et al. Cellular Senescence Promotes Adverse Effects of Chemotherapy and Cancer Relapse. Cancer Discov. 2017;7(2):165–176. [PubMed: 27979832]

62. Milanovic M, Fan DNY, Belenki D, et al. Senescence-associated reprogramming promotes cancer stemness. Nature. 2018;553(7686):96–100. [PubMed: 29258294]

63. Li M, You L, Xue J, Lu Y. Ionizing Radiation-Induced Cellular Senescence in Normal, Non-transformed Cells and the Involved DNA Damage Response: A Mini Review. Front Pharmacol. 2018;9:522. [PubMed: 29872395]

64. He Y, Thummuri D, Zheng G, et al. Cellular senescence and radiation-induced pulmonary fibrosis. TranslRes. 2019;209:14–21.

Implications:

This work exploits a key genomic hallmark of HPV- HNSCC (*CDKN2A* disruption) using palbociclib to induce BCL-xL dependent senescence, which subsequently causes the cancer cells to be vulnerable to the senolytic agent, navitoclax.

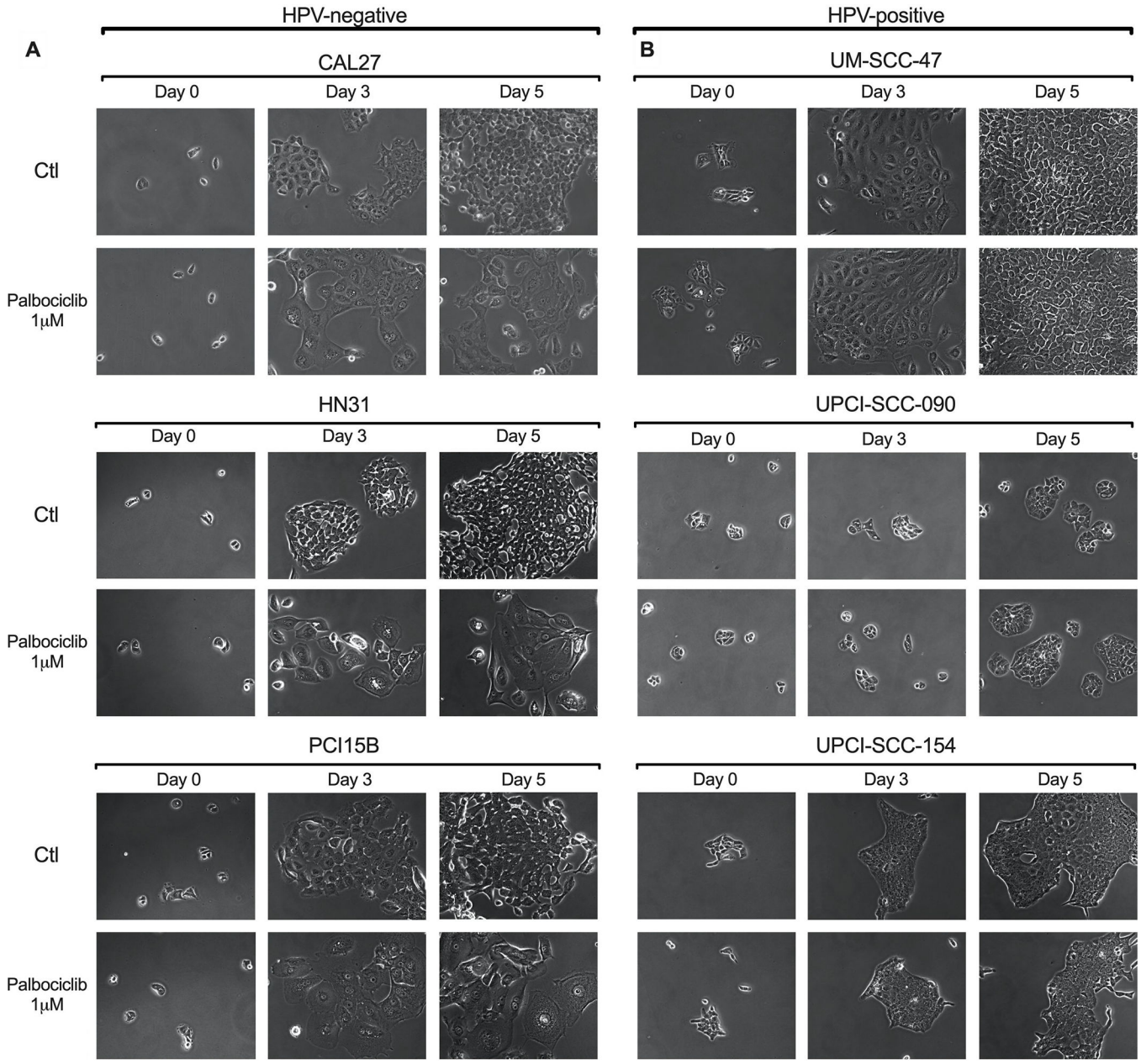

Figure 1.

Cell morphology observed via light microscopy in HNSCC lines after incubation with palbociclib. 24 hours following plating, cells were incubated in 1μM palbociclib or left untreated (controls). Images were taken on day of drug addition (Day 0), as well as Day 3, and Day 5 of drug incubation. Representative images, at the same magnification throughout, at each time point are shown for both palbociclib treated and untreated control groups. Data presented for HPV- HNSCC lines (**A**) demonstrate flattening and enlargement, as well as decreased numbers, all characteristic features of senescence morphology, while HPV+ HNSCC lines appear similar to controls (**B**).

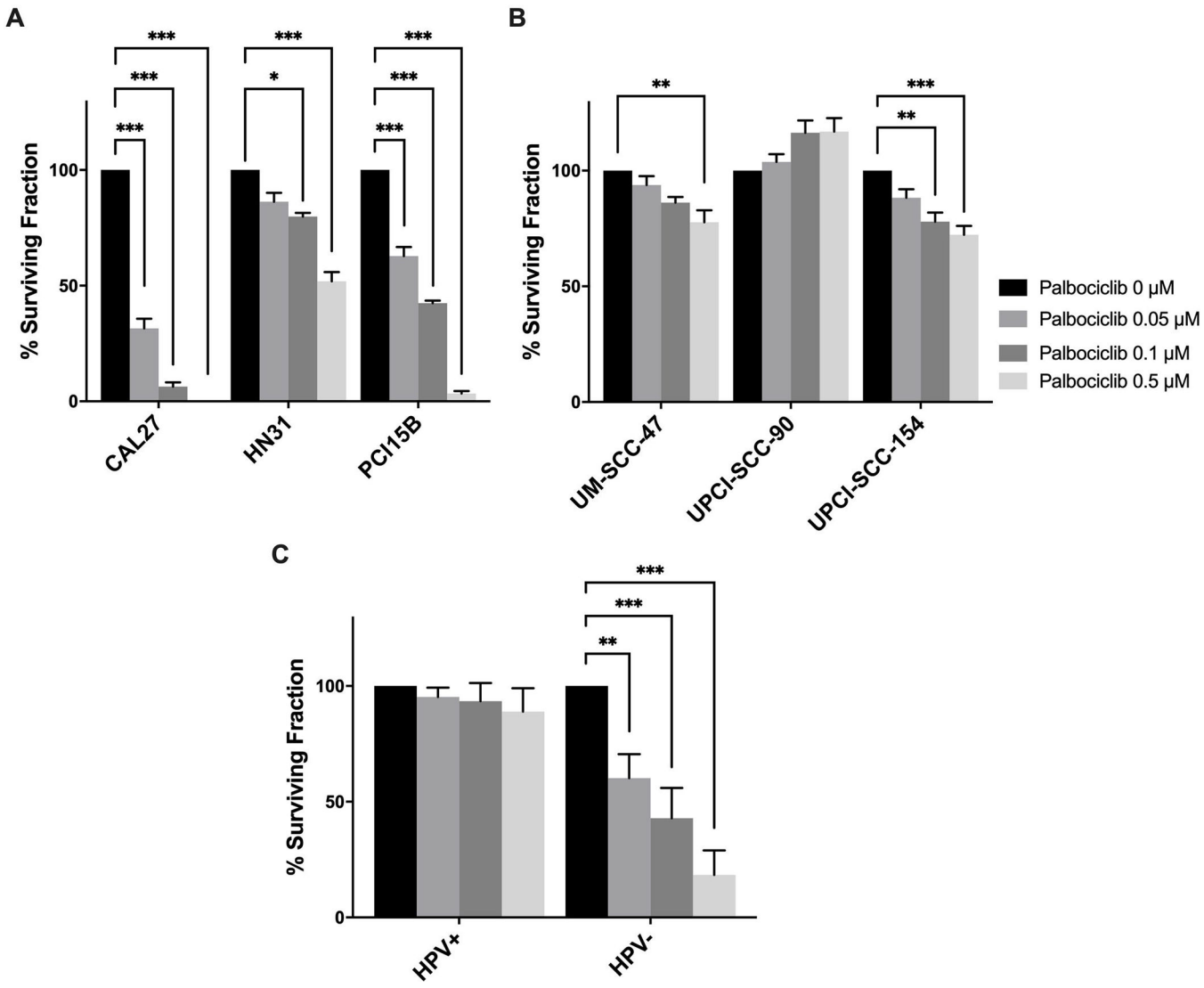

Figure 2.

Clonogenic survival of head and neck squamous cell carcinoma (HNSCC) lines following treatment with increasing concentrations of palbociclib. Cells were incubated with 0.05, 0.1, and 0.5 μM palbociclib for 10 days (HPV- lines) or 14 days (HPV+ lines), and then assessed for colony formation. Colonies were counted and surviving fraction was standardized against the untreated control. Percent surviving fraction of each cell line is presented for each palbociclib concentration as indicated. Data presented as mean ± standard error of the mean (SEM) from three biological replicates performed on different days, with three technical replicates per biological replicate. Data are presented for HPV- (**A**) and HPV+ (**B**) HNSCC lines, as well as a pooled analysis comparing HPV+ and HPV- lines (**C**). Statistical significance is indicated: * if $p < 0.05$, ** if $p < 0.01$, *** if $p < 0.001$, comparing treatment groups with control group as determined by ANOVA and Dunnett's multiple comparisons test (**A**) and (**B**), and a pooled analysis comparing each treatment condition with control using a matched paired t-test (**C**).

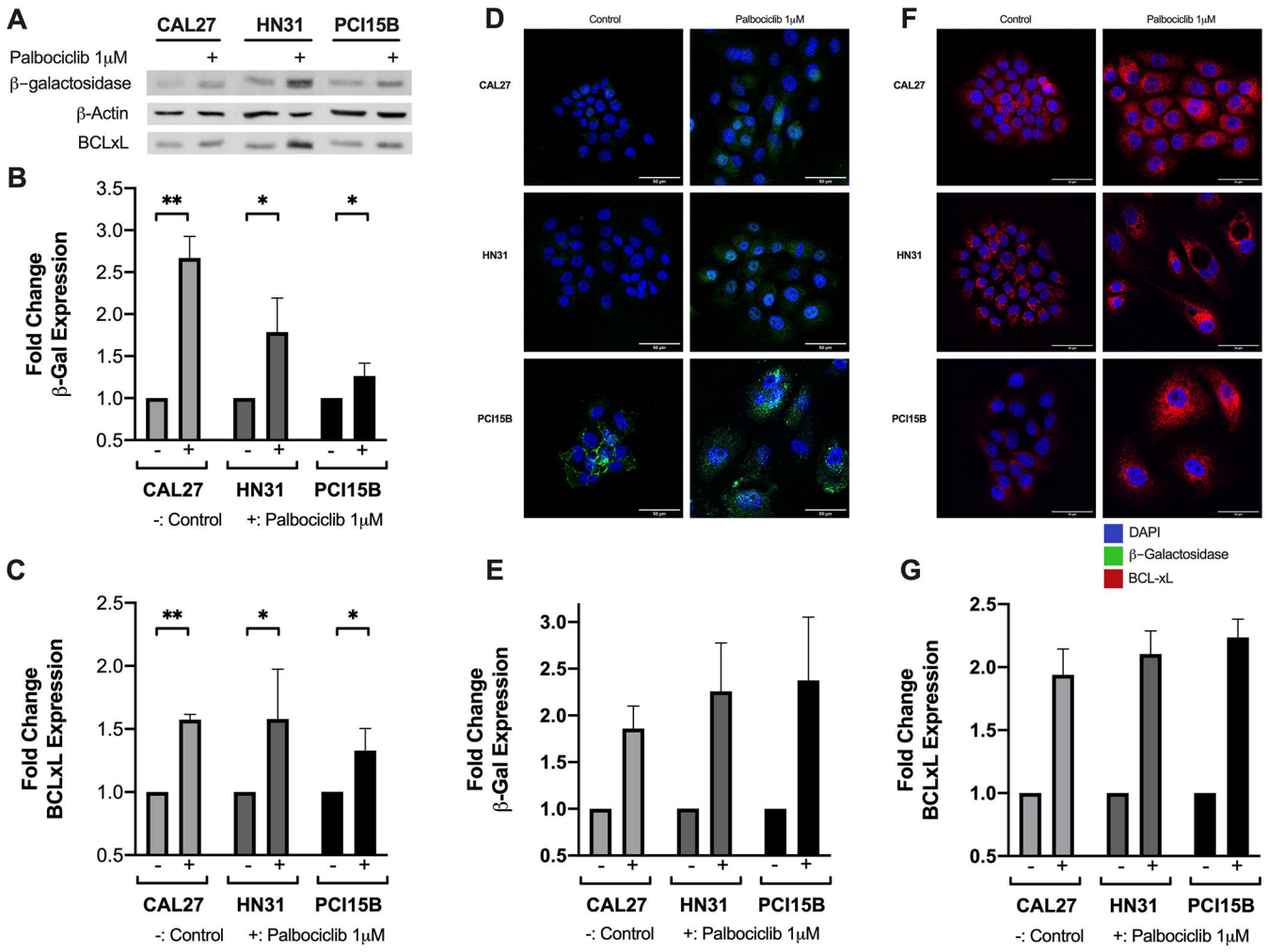

Figure 3.

β-galactosidase and BCL-xL expression following palbociclib treatment among the panel of HPV- head and neck squamous cell carcinoma (HNSCC) lines. Representative western blot showing protein expression for β-galactosidase (β-gal), BCL-xL, and β-actin, with (+) designating treatment condition with 1 μM palbociclib (**A**). Fold changes shown in β-gal (**B**) and BCL-xL (**C**) relative to untreated controls. HPV-lines were exposed to 1 μM palbociclib for 24 hours prior to immunofluorescent staining. Representative epifluorescence microscopy images shown for both β-gal (**D**) and BCL-xL (**F**), with DAPI in blue, β-gal in green, and BCL-xL in red. Fold changes in β-gal (**E**) and BCL-xL (**G**) relative to untreated controls. Scale bar indicates 50μm. Data in (**B**) and (**C**) displayed as mean ± standard deviation; data in (**E**) and (**G**) displayed as mean ± standard error of the mean. All data represent at least three biological replicates performed on different days. Statistical significance is indicated: * if $p < 0.05$, ** if $p < 0.01$, comparing treatment group with control group using unpaired t-test.

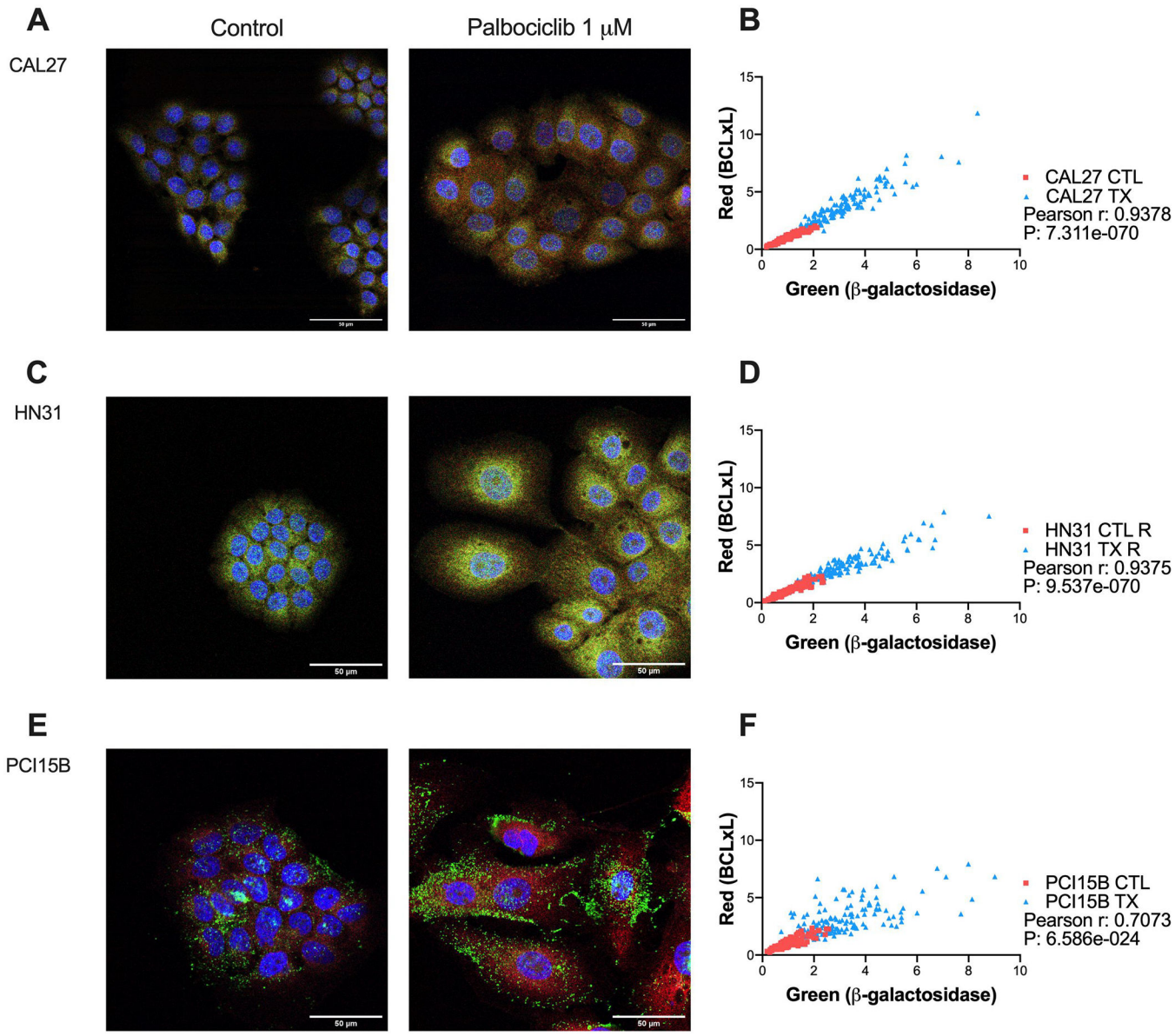

Figure 4.

Co-expression of β-galactosidase and BCL-xL following palbociclib treatment among the panel of HPV- head and neck squamous cell carcinoma (HNSCC) lines. Cells were exposed to 1 μM palbociclib for 24 hours before immunofluorescent staining. Representative confocal microscopy images for control and treatment conditions shown (**A, C, E**), with DAPI in blue, β-gal in green, and BCL-xL in red. Co-expression analysis for each cell line (**B, D, F**), with every point on the graph representing the pixel intensity per cell for one cell for β-gal and BCL-xL, and overall illustrating strong correlation for all lines. Scale bar indicates 50μm. Data displayed from three biological replicates performed on different days.

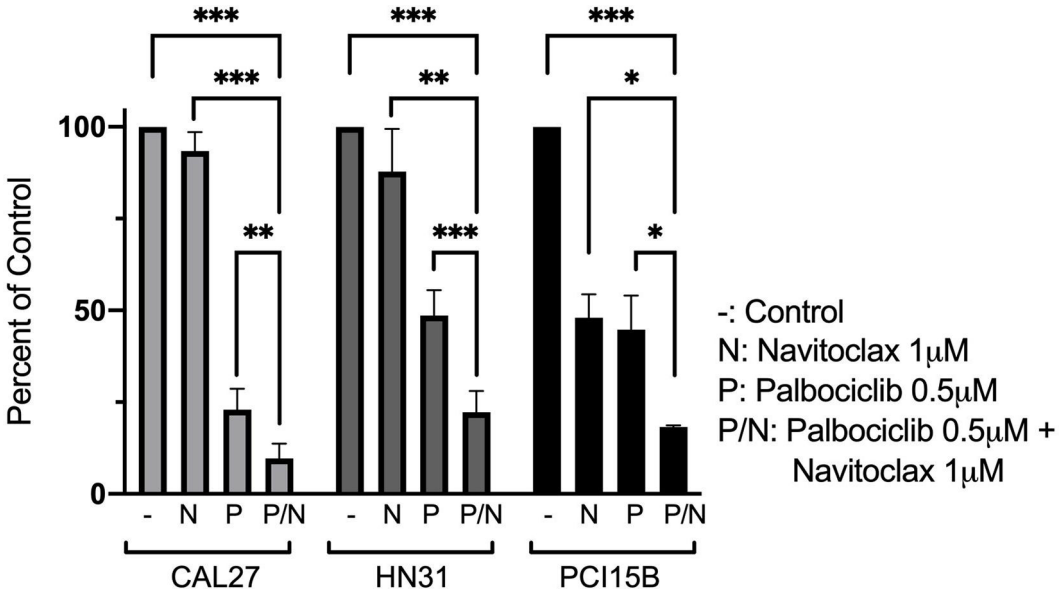

Figure 5.

Cell viability assay following treatment with palbociclib, navitoclax, or combination of the two agents among the panel of HPV- head and neck squamous cell carcinoma (HNSCC) cell lines. Cells were exposed to 0.5 μM palbociclib, 1 μM navitoclax, or combination of the two agents for 6 days prior to harvest. Data displayed as mean ± standard error of the mean (SEM) from three biological replicates performed on different days, with three technical replicates per biological replicate. Statistical significance is indicated: * if $p < 0.05$, ** if $p < 0.01$, *** if $p < 0.001$, comparing combination treatment group with control group, as well as comparing each single treated group with the combination treatment group, all using two-tailed paired t-tests.

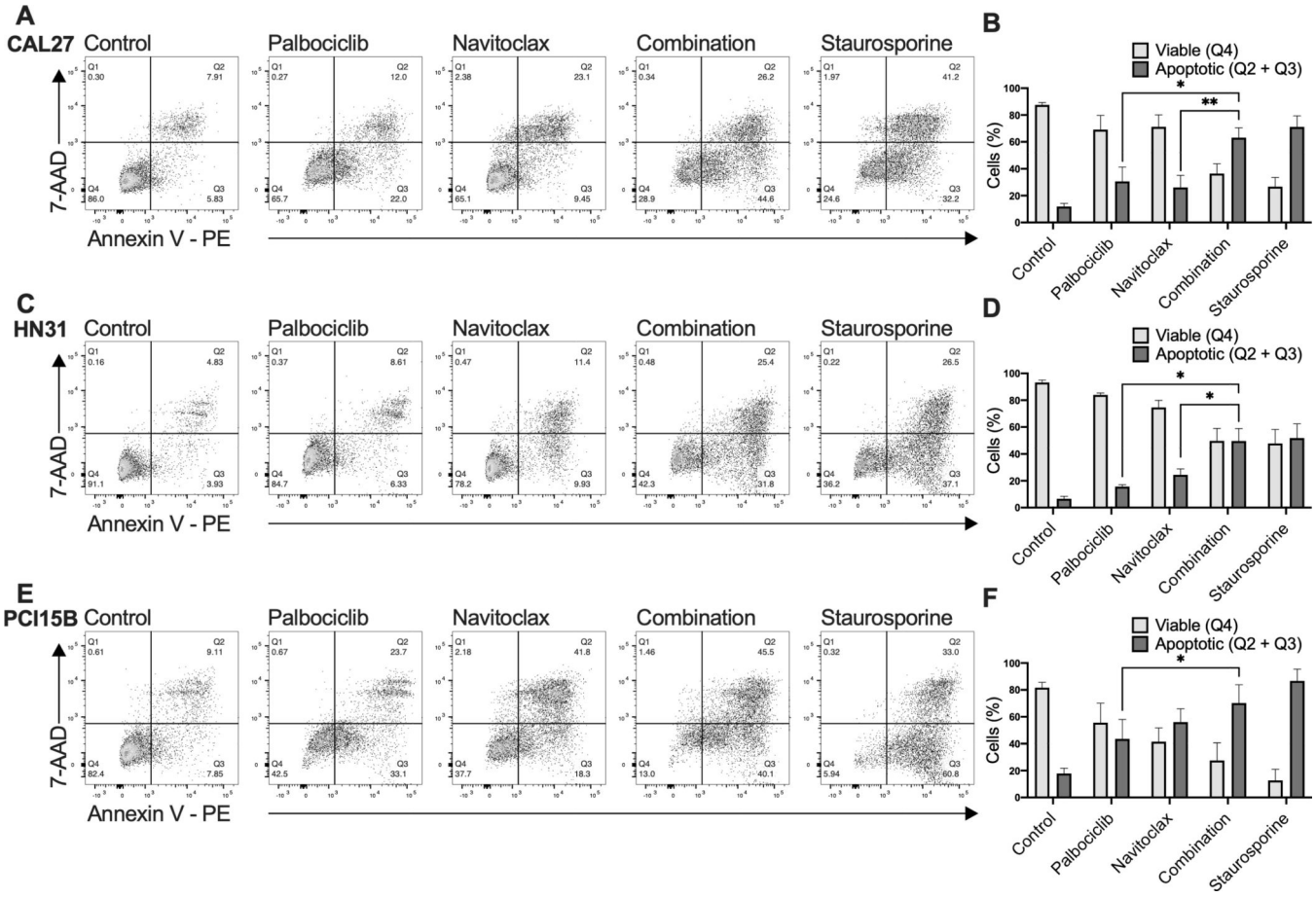

Figure 6.

Annexin V apoptosis assay following treatment with palbociclib, navitoclax, or combination of the two agents among the panel of HPV- head and neck squamous cell carcinoma (HNSCC) cell lines. Cells were exposed to 0.5 μM palbociclib, 1 μM navitoclax, or combination of the two agents, or 1 μM staurosporine (positive control). Cells were harvested after 72 hours and analyzed by flow cytometry. Representative flow cytometry analysis graphs (**A, C, E**) illustrate staining with 7-AAD and Annexin V-PE under each drug treatment condition for each line. Proportions of viable and apoptotic cells in each drug treatment condition for each line (**B, D, F**), with data displayed as mean ± standard deviation from three biological replicates performed on different days. Statistical significance is indicated: * if $p < 0.05$, ** if $p < 0.01$, comparing combination treatment group with each single agent all using two-tailed paired t-tests.

Table 1.

Head and Neck Squamous Cell Carcinoma Cell Lines

Cell Line	HPV Status	Site of Origin
CAL27	Negative	Oral Cavity
HN31	Negative	Pharynx*
PCI15B	Negative	Pharynx*
UM-SCC-47	Positive	Oral Cavity
UPCI-SCC-090	Positive	Oral Cavity
UPCI-SCC-154	Positive	Oral Cavity

Abbreviations:
HPV: Human papillomavirus

*Metastatic Lymph Node derived